Increased glycosphingolipid levels in serum and aortae of apolipoprotein E gene knockout mice

Brett Garner,[1,*] David A. Priestman,[1,*] Roland Stocker,[†] David J. Harvey,[*] Terry D. Butters,[*] and Frances M. Platt[2,*]

Oxford Glycobiology Institute,[*] Department of Biochemistry, University of Oxford, South Parks Road, Oxford OX1 3QU, UK; and Biochemistry Group,[†] Heart Research Institute, Sydney, 2050 N.S.W., Australia

Abstract **The apolipoprotein E gene knockout (apoE$^{-/-}$) mouse develops atherosclerosis that shares many features of human atherosclerosis. Increased levels of glycosphingolipid (GSL) have been reported in human atherosclerotic lesions; however, GSL levels have not been studied in the apoE$^{-/-}$ mouse. Here we used HPLC methods to analyze serum and aortic GSL levels in apoE$^{-/-}$ and C57BL/6J control mice. The concentrations of glucosyl ceramide (GlcCer), lactosyl ceramide (LacCer), GalNAcβ1-4Galβ1-4Glc-Cer (GA2), and ceramide trihexoside (CTH) were increased by approximately 7-fold in the apoE$^{-/-}$ mouse serum compared with controls. The major serum ganglioside, *N*-glycolyl GalNAcβ1-4[NeuNAcα2-3]Galβ1-4Glc-Cer (*N*-glycolyl GM2), was increased in concentration by approximately 3-fold. A redistribution of GSLs from HDL to VLDL populations was also observed in the apoE$^{-/-}$ mice. These changes were accompanied by an increase in the levels of GSLs in the aortic sinus and arch of the apoE$^{-/-}$ mice. The spectrum of gangliosides present in the aortic tissues was more complex than that found in the lipoproteins, with the latter represented almost entirely by *N*-glycolyl GM2 and the former comprised of NeuNAcα2-3Galβ1-4Glc-Cer (GM3), GM2, *N*-glycolyl GM2, GM1, GD3, and GD1a. In conclusion, neutral GSL and ganglioside levels were increased in the serum and aortae of apoE$^{-/-}$ mice compared with controls, and this was associated with a preferential redistribution of GSL to the proatherogenic lipoprotein populations. The apoE$^{-/-}$ mouse therefore represents a useful model to study the potential role of GSL metabolism in atherogenesis.**—Garner, B., D. A. Priestman, R. Stocker, D. J. Harvey, T. D. Butters, and F. M. Platt. **Increased glycosphingolipid levels in serum and aortae of apolipoprotein E gene knockout mice.** ***J. Lipid Res.*** **2002.** 43: **205–214.**

Supplementary key words apoE gene knockout • ganglioside analysis • atherosclerosis

The development of the apoE gene knockout (apoE$^{-/-}$) mouse has provided a widely used animal model of human atherosclerosis (1). The apoE$^{-/-}$ mouse spontaneously develops hypercholesterolemia on a standard chow diet, and this is associated with a striking increase in cholesterol-rich, βVLDL-like, remnant lipoproteins and a decreased concentration of HDL (2, 3). The morphology of atherosclerotic lesions that develop at specific sites of the apoE$^{-/-}$ mouse aorta has also been studied in detail and found to share similarities with human atherosclerosis at all stages of lesion development (4–6). At 3 weeks of age, signs of lesion development (lipid retention) are detectable in the intimal layer of the aortic arch, and by 5 months of age, foam cells accumulate in the aortic sinus and fatty streaks are present in the proximal aorta (3–6). After 9 months, complex atherosclerotic lesions with fibrous caps develop and the lesion size, as well as the rate of formation, is exacerbated when the apoE$^{-/-}$ mouse is fed a high fat diet (0.15% cholesterol and 21% fat) (4, 5).

In addition to the morphological similarities of atherosclerotic lesions in the apoE$^{-/-}$ mouse and humans, several pathophysiological processes thought to contribute to atherosclerosis in humans also occur in the apoE$^{-/-}$ mouse. These include infiltration of CD4^{+} T cells into the artery wall (7) and the partial oxidation of plasma lipoproteins and artery wall components (8–10). Inter-crossing of apoE$^{-/-}$ mice with P-selectin-deficient mice, immunodeficient (scid/scid) mice, or mice containing the osteopetrotic (*op*) mutation in the macrophage colony stimulating factor gene has been used to reveal the potential proatherogenic roles of P-selectin, CD4+ T cells, and macrophages, respectively, in lesion development (11–13). The apoE$^{-/-}$ mouse also provides a model to assess pharmaceutical and dietary interventions that could be potentially anti-atherogenic in humans (1, 14, 15).

Abbreviations: apoE$^{-/-}$, apolipoprotein E gene knockout; 2-AB, 2-aminobenzamide; CTH, ceramide trihexoside Galα1-4Galβ1-4Glc-Cer; GA2, GalNAcβ1-4Galβ1-4Glc-Cer; GD1a, NeuNAcα2-3Galβ1-3GalNAcβ1-4[NeuNAcα2-3]Galβ1-4Glc-Cer; GD3, NeuNAcα2-8NeuNAcα2-3Galβ1-4Glc-Cer; gGM2, GalNAcβ1-4[NeuNGcα2-3] Galβ1-4Glc-Cer; GlcCer, glucosyl ceramide; GM1, Galβ1-3GalNAcβ1-4[NeuNAcα2-3]Galβ1-4Glc-Cer; GM2, GalNAcβ1-4[NeuNAcα2-3] Galβ1-4Glc-Cer; GM3, NeuNAcα2-3Galβ1-4Glc-Cer; GSL, glycosphingolipid; G.U., glucose unit; HPTLC, high performance thin layer chromatography; LacCer, lactosyl ceramide Galβ1-4Glc-Cer; MALDI-CID, matrix-assisted laser desorption-collision induced dissociation; MS, mass spectrometry; NP-HPLC, normal phase high-performance liquid chromatography; Q-Tof, quadrupole-time-of-flight; TC, total cholesterol.

[1] These authors contributed equally to this work.
[2] To whom correspondence should be addressed.
e-mail: fran@glycob.ox.ac.uk

Glycosphingolipid (GSL) metabolism represents another potential contributing factor in human atherosclerosis that has not been studied in a relevant mouse model. The plasma GSLs are based on the glucosyl ceramide (GlcCer) core structure (16), reflecting their site of synthesis in the liver (17). In humans, more than 90% of plasma GSLs are transported in lipoproteins, with approximately 66% associated with LDL (18). Although GSL exchange between LDL and HDL has been observed in vitro (19), the factors that may regulate such transfers in plasma remain unknown. It is well recognized that both neutral GSLs and gangliosides accumulate in human atherosclerotic tissue and that there is a positive correlation between plasma cholesterol and GSL concentrations in humans (20–29). Several hypotheses have been proposed to account for a direct proatherogenic effect of specific GSLs. Lactosyl ceramide (LacCer) induces smooth muscle cell proliferation in vitro (30), and other studies show that ganglioside NeuNAcα2-3Galβ1-4Glc-Cer (GM3) can markedly accelerate LDL uptake by macrophages, leading to the generation of lipid-laden foam cells (31). A recent study has revealed an important role for GM3 and GD3 in the adhesion of platelets to sites of atherosclerotic lesion formation (32). In general terms, both neutral and acidic GSLs could have myriad effects related to atherogenesis, including regulation of cellular signaling (33), activation (34), recognition (35), glucose metabolism (36), differentiation (37), fibrinolytic activity (38), phagocytosis (39), nitric oxide production (40), surface expression of GPI-anchored proteins (41), and response to growth factors (42).

Although many of the biological activities of GSLs could play a role in atherogenesis, lack of a suitable animal model has restricted the investigation of these pathways in vivo. The present work examined whether the apoE$^{-/-}$ mouse exhibits any of the changes in GSL levels that are associated with human atherosclerosis, with the aim of assessing the potential utility of this animal model for investigating the role of GSLs in atherogenesis.

MATERIALS AND METHODS

Materials

Acetonitrile (chromosolv) and hexane were from Riedel-de Haen (Haen, Germany). Methanol, chloroform, and KBr were from BDH (Poole, UK). Acetone was from Fisher Chemicals (Loughborough, UK). Phosphate buffered saline was prepared using Oxoid (Basingstoke, UK) tablets. Ceramide glycanase (E.C. 3.2.1.123) was from Calbiochem (La Jolla, CA).

Animals and diet

C57BL/6J mice and homozygous apoE$^{-/-}$ mice (kindly provided by Peter Carmeliet, Katolieke Universiteit Leuven, Belgium) were fed a standard chow diet (RM1 diet, Special Diet Services, Witham, UK) ad libitum for 26 weeks. Serum samples were then collected and the hearts and arterial trees carefully dissected as described previously (10) under a Zeiss Stemi 2000 dissecting microscope (Carl Zeiss, Munich, Germany). Gross lesion formation was assessed by microscopic examination of the intact formalin-fixed proximal aorta and sections of the aortic sinus. Images were digitally captured using an Axioscop-2 plus microscope and Axiovision software (Carl Zeiss). The presence of atherosclerosis in the aortic sinus was determined in tissue sections stained with Weigert's hematoxylin-van Gieson's stain (43).

Isolation of lipoprotein fractions

Murine lipoprotein fractions were isolated by density ultracentrifugation, essentially as described previously (44). Briefly, serum samples were pooled from two mice for each lipoprotein preparation, and 1 ml of each of the pooled samples was adjusted to a density of 1.24 g/ml with KBr. The lipoprotein fractions were then separated by density ultracentrifugation (417,000 *g*, 4 h, 15°C) using a TL-100 bench-top ultracentrifuge with a TLA-100.4 rotor (Beckman, Palo Alto, CA) (45). As mouse serum contains a low concentration of carotenoids, the lipoprotein bands are difficult to localize after ultracentrifugation. The positions of the murine HDL, LDL/IDL, and VLDL fractions were, therefore, estimated by comparison with human plasma samples that were treated in parallel. Because the apoE$^{-/-}$ mouse serum contains a continuum of particles in the LDL/IDL density range (3, 44), these fractions were pooled in the present study. The following volumes were collected from each of the 5 ml centrifuge tubes, beginning from the top of the tube: 1.0 ml (VLDL), 1.5 ml (LDL/IDL), 0.3 ml (discarded), 1.0 ml (HDL), and the remaining fraction in the bottom of the tube (1.2 ml) was discarded. Using this approach, approximately 90% of the serum cholesterol was recovered in the lipoprotein fractions.

The cholesterol and triglyceride concentrations of the serum samples and the isolated lipoprotein fractions were determined by enzymatic methods using Randox assay kits (Randox Crumlin, Antrim, UK).

Analysis of serum and lipoprotein GSL concentrations

Forty microliters of serum or lipoprotein fraction was extracted in 4 ml chloroform-methanol (2:1, v/v) by 15 s vigorous shaking in a glass tube followed by 15 min sonication in a water bath at 22°C. The samples were then placed on ice for approximately 2 min and subsequently centrifuged at 4000 rpm for 10 min at 4°C in a Beckman Allegra 6R centrifuge. The supernatant (3.6 ml) was removed and evaporated to dryness under vacuum (Howe, GyroVap). The crude lipid fraction was redissolved in 200 μl chloroform and passed over a silicic acid column prepared by adding 1 ml of silicic acid-chloroform suspension (10%, w/v) to a plastic cartridge containing a frit at the outlet. The lipid fractions were eluted from the column in the following order: 5 ml chloroform was used to elute neutral lipids (predominantly cholesteryl esters and triglycerides); 1.8 ml of methanol-acetone (1:9, v/v) was then used to elute neutral glycolipids (predominantly LacCer and GlcCer); and the ganglioside fraction (predominantly GM2) was eluted with 1.8 ml methanol. The neutral and ganglioside fractions were evaporated to dryness under vacuum and redissolved in 50 μl of 50 mM sodium actetate buffer (pH 5) containing 1 mg/ml sodium cholate and 0.1 units ceramide glycanase. The mixtures were then incubated in a sterile atmosphere at 37°C for 18 h to release the carbohydrate moiety from ceramide (46), passed over an Oasis HLB cartridge (Waters), fluorescently labeled with 2-aminobenzamide (2-AB) (47), and analyzed by normal phase high-performance liquid chromatography (NP-HPLC) as described below. The incubation conditions have been previously optimized for complete GSL hydrolysis as assessed by thin layer chromatography and scanning densitometry (46). The quantification of GSLs was achieved by comparison with a commercial GM3 standard (Sigma) and was accurate over a linear range from 1 pmol to at least 10 μmol. Recovery of exogenously added GM3 to serum samples was assessed in three experiments and found to be 75 ± 10% (mean ± SE). In the case of serum GlcCer analysis, free glucose was found to interfere with the HPLC assay. Consequently, the serum samples were pooled (up to five mice to give

a sample volume of 0.5 ml), and the isolated GSLs analyzed by high-performance thin layer chromatography (HPTLC). Briefly, samples were dissolved in 5 μl chloroform-methanol (2:1, v/v) and loaded on Silica Gel 60 HPTLC plates (Merck, Damstadt, Germany) with GlcCer, LacCer, ceramide trihexoside (CTH), and globoside run in parallel lanes (Matreya, Pleasant Gap, PA). The samples were then separated in chloroform-methanol-water (65:25:4, v/v/v) until the solvent front reached the top of the plate. The plates were air-dried and GSLs visualized by spraying with 0.2% (v/v) orcinol in 1 M sulphuric acid, followed by drying for 10 min at 80°C. The plates were scanned and GlcCer was quantified densitometrically (NIH Image 1.62 software).

Measurement of aortic GSL concentrations

Sections of the aortic sinus (sectioned either side of the aortic valve and carefully trimmed of cardiac muscle) and proximal aorta (dissected from the aortic root to just past the left subclavian artery before the first single intercostal artery) were weighed, then extracted in chloroform-methanol as follows. Aorta samples were freeze-dried overnight, then chopped finely with bow-spring scissors in 50 μl chloroform-methanol (2:1, v/v). The scissors were then rinsed with 150 μl chloroform-methanol that was added to the solvent extract. The samples were then sonicated in a water bath for 3 h prior to centrifugation at 10,000 *g* for 5 min. The supernatant was retained and the pellet re-extracted for 2 h on a vibrating shaker. The samples were centrifuged as above, the supernatants were pooled and then dried under a stream of nitrogen. The dried samples were then resuspended in 0.5 ml chloroform, and the lipid fractions were separated by silicic acid column chromatography as described above. The isolated neutral and ganglioside fractions were then subjected to ceramide glycanase treatment, and the recovered glycans were labeled with 2-AB and analyzed by NP-HPLC as described below.

Analysis of 2-AB labeled glycans by NP-HPLC

HPLC separations were performed on a 0.46 × 25 cm Glycosep-N chromatography column (Oxford GlycoSciences) using low-salt conditions, and structures were assigned to the glycans based on their elution positions [converted to glucose unit (G.U.) values] as compared with known G.U. values for previously characterized glycans (29, 47, 48). A compound isolated from apoE$^{-/-}$ mouse aortae (and eluting from the NP-HPLC column very close to the car-

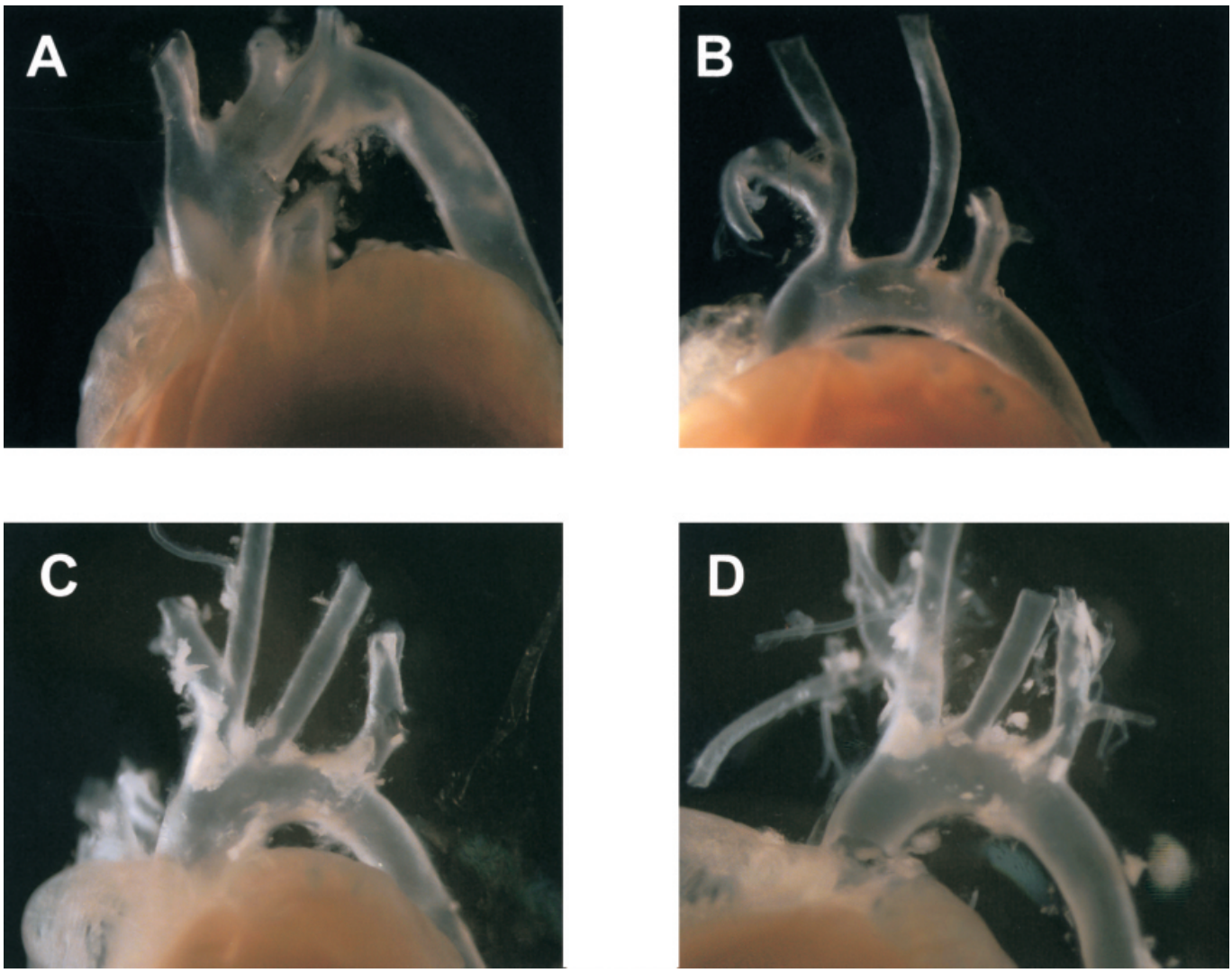

Fig. 1. Gross morphology of proximal aortae. C57BL/6J (A and B) and apolipoprotein E gene knockout (apoE$^{-/-}$) (C and D) mice were maintained on a normal chow diet for 6 months, after which their hearts and aortae were perfusion-fixed with formalin, dissected, and photographed under a dissecting microscope (original magnification 6.5×). The presence of atherosclerotic lesions (whitish plaques) are clearly observed at the inner curvature of the aorta and the branch points in the apoE$^{-/-}$ mice (C and D).

bohydrate moiety of glycolyl GM2 but with a G.U. value of 3.77) appeared to be the carbohydrate moiety of the lactone form of glycolyl GM2, based on its co-elution with synthetic *N*-glycolyl GM2 lactone. The latter compound was generated by treating purified glycolyl GM2 (derived from apoE$^{-/-}$ serum) with 1 N acetic acid for 4 days at 22°C according to an established method (49). We were unable to recover sufficient material from the aortic tissues to conduct structural analysis by mass spectrometry (MS). Lactonization of gangliosides has been proven to occur in vivo (50).

Analysis of 2-AB-labeled glycans by matrix-assisted laser desorption-collision induced dissociation MS

A fragmentation spectrum of 2-AB-labeled GM2 was obtained with a tandem quadrupole-time-of-flight (Q-Tof) mass spectrometer fitted with an experimental matrix-assisted laser desorption ion (MALDI) source (51) [Micromass (UK) Ltd, Manchester]. The sample, in 1 μl of water, was mixed with 2,5-dihydroxybenzoic acid (0.9 μl of a saturated solution in acetonitrile) on the MALDI probe and allowed to dry. The probe was introduced into the ion source of the mass spectrometer via a vacuum lock and the laser was fired at 20 Hz. Signals were accumulated for 5 s for each spectrum, and positive ion spectra were accumulated until a satisfactory signal-noise ratio was obtained. For MS/MS collision induced dissociation (CID) spectra, the precursor ion ($[M+H]^+$) was selected with a mass window of about 3 Da, argon was used as the collision gas, and the collision energy was set to record fragments across the entire mass range.

Statistical analysis

Statistical significance was determined using the 2-tailed *t*-test for unpaired data. A *P* value of <0.05 was considered significant.

RESULTS

Confirmation of the presence of atherosclerotic lesions in apoE$^{-/-}$ mice

Previous studies have shown that apoE$^{-/-}$ mice develop atherosclerotic lesions in the proximal aorta and aortic sinus after 5 months on a normal chow diet (3). We confirmed the presence of atherosclerotic disease in the present study of 6-month-old apoE$^{-/-}$ mice. **Figure 1** shows that atherosclersotic lesions were visible at the inner curvature of the aortic arch and at the principal branches of the aorta in the apoE$^{-/-}$ mice but not in C57BL/6J wild-type mice. The lesions were macroscopically visible after tissue fixation, even without histological staining. The presence of atherosclerosis in the aortic root was also confirmed by histological examination of three apoE$^{-/-}$ mice. **Figure 2** illustrates a marked intimal lipid accumulation in the aortic sinus, again confirming earlier studies (3). Having confirmed the presence of atherosclerotic disease in the apoE$^{-/-}$ mice, we conducted a detailed examination of the GSLs present in the sera and aortae of apoE$^{-/-}$ and C57BL/6J mice.

Serum GSL, cholesterol, and triglyceride concentrations

A novel technique was used to determine serum GSL composition and concentration. This procedure was based on the enzymatic removal of the ceramide moieties of GSLs followed by HPLC separation of the remaining fluorescently labeled glycan moieties (48). The method is ideal for mouse studies, as only 40 μl of serum is required for GSL analysis. Three prominent neutral GSLs were analyzed in mouse serum. These were identified as LacCer, GA2, and CTH by comparison of the G.U. values of their respective glycans with those of known standards and previously characterized GSLs derived from mouse liver and human plasma (**Fig. 3**). GlcCer is also present in mouse serum; however, due to contamination of the samples with glucose, reliable measurements of this GSL could not be achieved using the HPLC method. Serum GlcCer was, therefore, analyzed by HPTLC (**Fig. 4**). Analysis of the ganglioside fraction of murine serum revealed a single

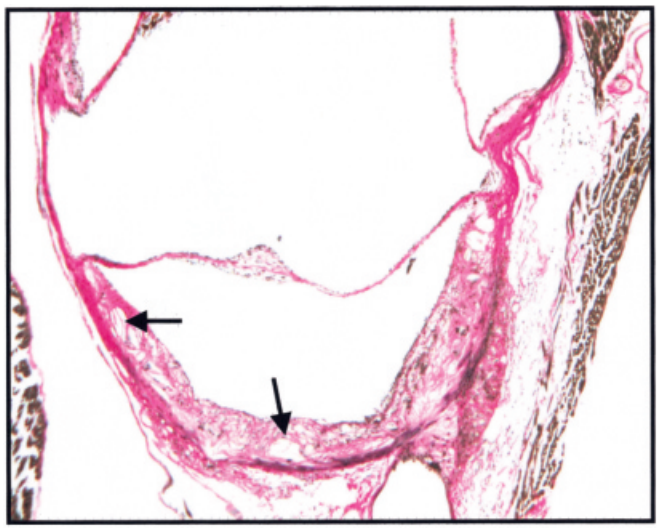

Fig. 2. Cross-section of the aortic root of an apoE$^{-/-}$ mouse heart. A section of the aortic root of a 6-month-old apoE$^{-/-}$ mouse heart stained with Weigert's hematoxylin-van Gieson's stain is shown (original magnification 10×). Lipid deposits and cholesterol crystals are present in the intima (indicated by arrows).

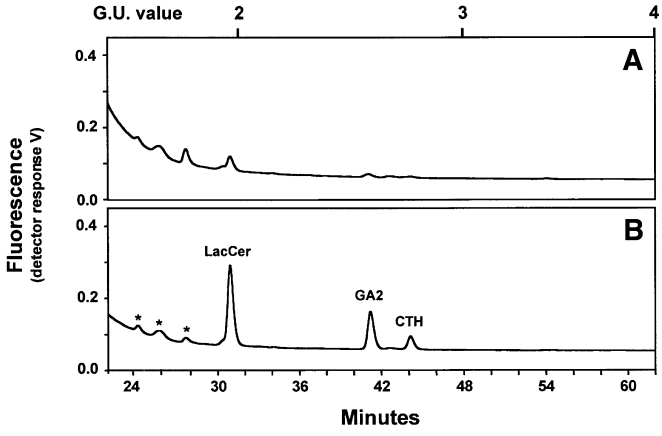

Fig. 3. HPLC analysis of neutral glycosphingolipids (GSL) isolated from mouse serum. GSLs were isolated by solvent extraction, and the glycan portion was released by ceramide glycanase treatment. The released glycan pool was then 2-aminobenzamide (2-AB) labeled and analyzed by normal phase HPLC (NP-HPLC). The major neutral GSLs were identified as lactosyl ceramide Galβ1-4Glc-Cer (LacCer), GalNAcβ1-4Galβ1-4Glc-Cer (GA2), and ceramide trihexoside Galα1-4Galβ1-4Glc-Cer (CTH). GSL profiles of representative C57BL/6J wild-type control (A) and apoE$^{-/-}$ (B) mice are shown. The asterisks indicate unidentified compounds.

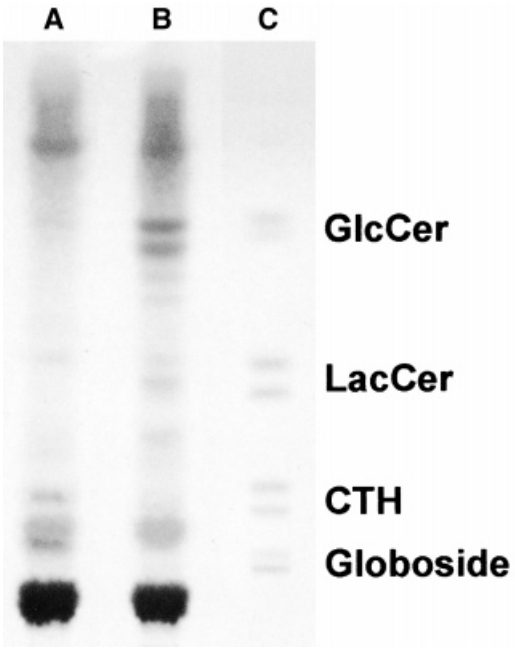

Fig. 4. HPTLC analysis of neutral GSLs isolated from pooled mouse sera. GSLs were isolated by solvent extraction from 500 μl of pooled mouse serum, separated on Silica Gel-60 HPTLC plates, and visualized by orcinol staining. Lane A: C57BL/6J control mice; lane B: apoE$^{-/-}$ mice; lane C: GSL standards are indicated.

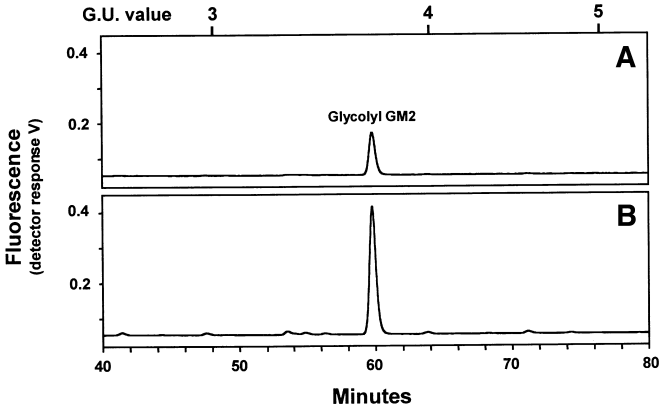

Fig. 5. HPLC analysis of gangliosides isolated from mouse serum. Gangliosides were isolated by solvent extraction, and the glycan portion was released by ceramide glycanase treatment. The released glycan pool was then 2-AB labeled and analyzed by NP-HPLC. The major ganglioside present was identified as GalNAcβ1-4[NeuNGcα2-3]Galβ1-4Glc-Cer (glycolyl GM2). Ganglioside profiles of representative C57BL/6J wild-type control (A) and apoE$^{-/-}$ (B) mice are shown.

dominant glycan species with a G.U. value of 3.67 (**Fig. 5**). The structure of this glycan was determined by MALDI-MS/MS to be GalNAcβ1-4[NeuNGcα2-3]Galβ1-4Glc (**Fig. 6**), indicating that the predominant murine serum ganglioside is GM2 containing *N*-glycolyl neuraminic acid. The presence of *N*-glycolylneuraminic acid was revealed by the loss of 307 mass units from the ions at *m/z* 973.5 and 770.4 (Fig. 6). *N*-acetylneuraminic acid would have produced losses of 291 mass units.

There were no differences in the spectra of either neutral GSLs or gangliosides present when the apoE$^{-/-}$ samples were compared with those from the C57BL/6J mice; however, serum GSL concentrations were increased in the apoE$^{-/-}$ mice (Figs. 3 and 5, compare chromatograms A and B). Serum GSL, cholesterol, and triglyceride concentrations in apoE$^{-/-}$ and C57BL/6J mice are summarized in **Table 1**. Cholesterol and triglyceride levels were significantly higher in the apoE$^{-/-}$ mice, in accordance with previous work (3). For the first time, we show that both the neutral GSL and ganglioside levels were also significantly higher in sera derived from the apoE$^{-/-}$ as compared with the C57BL/6J mice (Table 1). The higher ratio of ganglioside to neutral GSL and the absolute amounts of GSLs detected in the normal mice are in general agreement with studies conducted in mice and humans (18, 52–54).

Analysis of GSL fractional concentration in the major lipoprotein classes

The apoE$^{-/-}$ mouse displays a serum lipoprotein phenotype characterized by a redistribution of cholesterol from the HDL to the LDL, IDL, and VLDL fractions (3, 44). The increased plasma concentrations of cholesterol-rich, βVLDL-like particles are thought to be particularly atherogenic (3). **Figure 7** shows that in the apoE$^{-/-}$ mouse, approximately 90% of serum cholesterol is transported in the LDL, IDL, and VLDL fractions compared with approximately 24% of serum cholesterol in the C57BL/6J mouse. Figure 7 also shows that the fractional distribution of the GSLs throughout the lipoprotein classes is dramatically altered in the apoE$^{-/-}$ mouse where, collectively, approximately 80% of the major neutral and charged GSLs (LacCer and glycolyl GM2, respectively) are transported in the "pro-atherogenic" LDL, IDL, and VLDL fractions. Overall, the greatest change in the fractional distribution of GSLs in the different lipoprotein classes that we have isolated was a redistribution of both LacCer and glycolyl GM2 from HDL to VLDL (Fig. 7).

Analysis of GSL composition in aortic sinus and arch

In a final series of experiments, the neutral and acidic GSL composition of the aortic sinus and arch of both the apoE$^{-/-}$ and C57BL/6J mice was examined. The predominant neutral GSLs present were GlcCer and LacCer (**Fig. 8**). The ganglioside HPLC profiles were more complex, and we were able to identify six of the glycan moieties present (**Fig. 9**). The peak identified by the arrow in Fig. 9B co-eluted with the lactone form of the carbohydrate moiety of glycolyl GM2 (see Materials and Methods for further details). Because the lactone forms of GSL glycans are formed in vivo (50), it is possible that this peak (and possibly some of the other quantitatively minor peaks) represent the lactone forms of the ganglioside carbohydrates. **Table 2** indicates that both the neutral GSLs and gangliosides accumulated in the atherosclerostic lesions present in the aortic arch of the apoE$^{-/-}$ mouse. Although all of the values for LacCer were higher in the apoE$^{-/-}$ aortic arch samples, this was not sta-

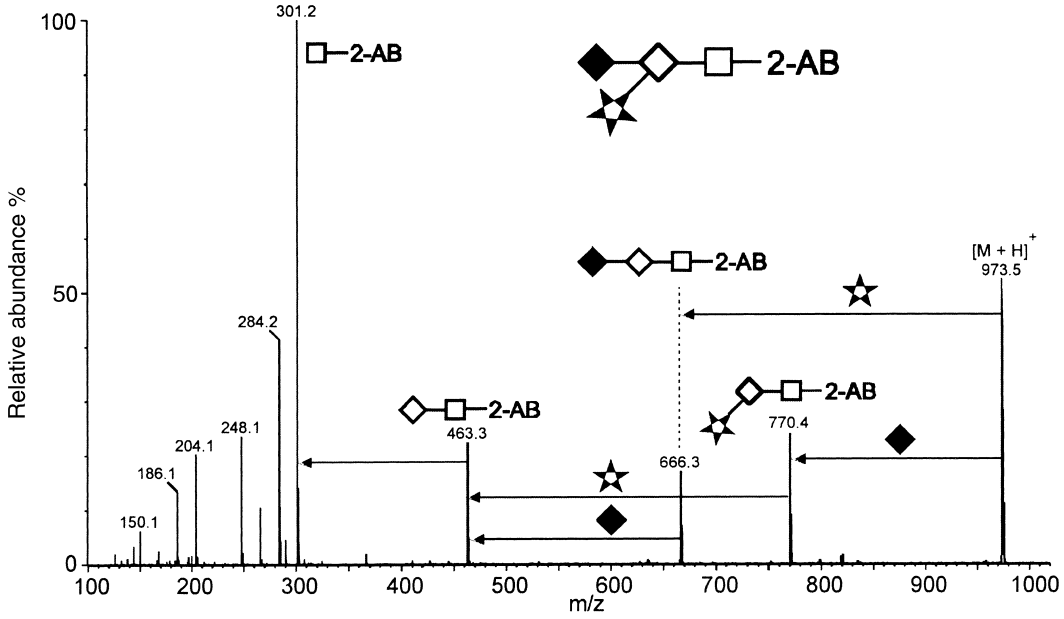

Fig. 6. Positive ion matrix-assisted laser desorption-collision induced dissociation (MALDI-CID) spectrum of the $[M+H]^+$ ion from the 2-AB derivative of GM2. The symbols above the arrows show the carbohydrate residues lost to give the major fragment ions. Symbols are: GalNAc (closed diamond), galactose (open diamond), glucose (open square), *N*-glycoylneuraminic acid (star). The presence of *N*-glycolylneuraminic acid is indicated by the losses of 307 mass units from the ions at *m/z* 973.5 and 770.4.

tistically significant due to the large variation observed (Table 2). The levels of neutral GSLs detected in the aortic sinus did not appear to be significantly higher in the apoE$^{-/-}$ mice. In the case of the gangliosides, the data are derived from the total of the areas under each of the HPLC peaks. In both the aortic arch and sinus, ganglioside levels were significantly increased in the apoE$^{-/-}$ mice (Table 2). When the increases in each of the known gangliosides were considered independently, it was clear that the largest increases were in glycolyl GM2 and GM1 for both the aortic sinus and arch (**Fig. 10**). Interestingly, the levels of GD3 were increased in the aortic sinus but not in the arch (Fig. 10).

TABLE 1. Concentrations of the major lipids and glycolipids of C57BL/6J and apoE$^{-/-}$ mouse serum

Analyte	n	C57BL/6J	ApoE$^{-/-}$	Fold↑
Cholesterol[a]	8	2.34 ± 0.12	13.69 ± 1.41[d]	5.9
Triglyceride[a]	8	1.35 ± 0.10	3.75 ± 0.37[d]	2.8
GM2[b]	3	13.3 ± 0.6	34.6 ± 3.4[e]	2.6
GlcCer[b,c]	Pooled	3	38	12.7
LacCer[b]	3	0.68 ± 0.02	4.14 ± 0.36[d]	6.1
GA2[b]	3	0.21 ± 0.05	1.61 ± 0.31[f]	7.7
CTH[b]	3	0.06 ± 0.01	0.55 ± 0.10[e]	9.2

GM2, GalNAcβ1-4[NeuNGcα2-3]Galβ1-4Glc-Cer; GlcCer, glucosyl ceramide; LacCer, lactosyl ceramide Galβ1-4Glc-Cer; GA2, GalNAcβ1-4Galβ1-4Glc-Cer; CTH, ceramide trihexoside Galα1-4Galβ1-4Glc-Cer. Where indicated, data are means ± SE, n = number of mice. Statistical significance was determined using the Student's *t*-test.

[a] Values are mmol/l.
[b] Values are μmol/l.
[c] Pooled sera from five mice in each group determined by HPTLC.
[d] $P < 0.001$.
[e] $P < 0.01$.
[f] $P < 0.05$.

DISCUSSION

Our results show, for the first time, that serum GSL levels are increased in the apoE$^{-/-}$ mouse model of atherosclerosis. The concentrations of neutral GSLs in C57BL/6J mice are somewhat lower than those observed in humans [e.g., LacCer concentrations of 1 μM and 5 μM, respectively (52, 53)], whereas the levels of the major ganglioside species (glycolyl GM2 for the mouse and GM3 for the human) are present at comparable concentrations (5 to 10 μM) (18, 54). In agreement with earlier work (54), we found that murine serum contained one predominant ganglioside, GM2 containing glycolyl neuraminic acid. In the apoE$^{-/-}$ mouse, the GSL levels were increased compared with those in the C57BL/6J mice; however, there were no qualitative differences in the GSL species identified. This is consistent with the idea that the increased serum GSL concentration is due to increased hepatic synthesis and not due to alterations in extra-hepatic tissue, as has been observed in mice bearing tumors (54, 55).

The accumulation of the most abundant ganglioside, GM3, in human atherosclerotic lesions is suggested to be due to both the direct accumulation of LDL-derived GM3 and locally synthesized GM3 (25). A detailed analysis of the fatty acid composition of GM3 derived from human atherosclerotic intima revealed a high content of C22–24 acids that are virtually absent from plasma LDL (20), thus

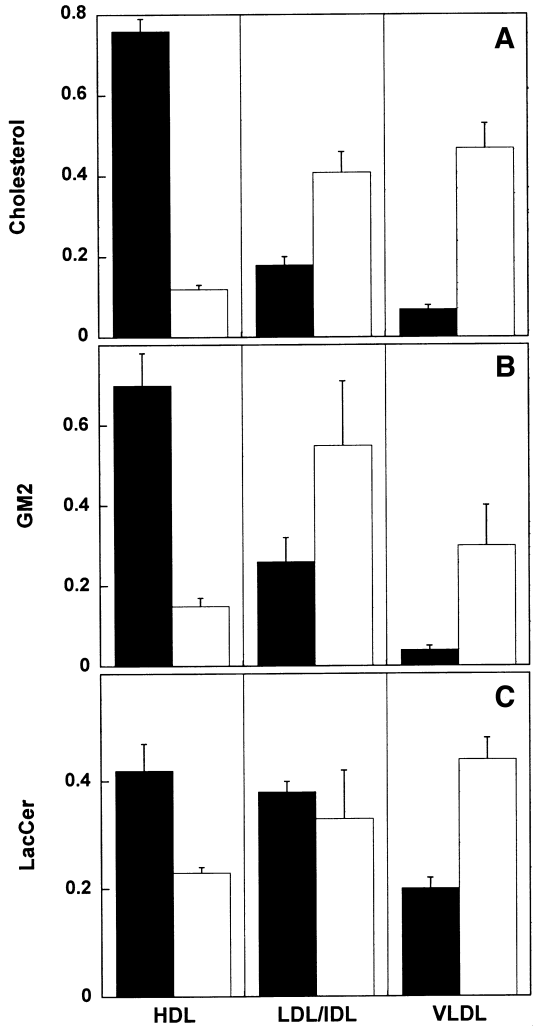

Fig. 7. Fractional distribution of cholesterol, GM2, and LacCer in the major lipoprotein classes. The major lipoprotein classes were isolated from murine serum by ultracentrifugation, and the cholesterol content was analyzed enzymatically. GSLs were isolated by solvent extraction, and their glycan moieties were released by ceramide glycanase treatment. The released glycan pool was then 2-AB labeled and analyzed by NP-HPLC. The values shown represent the fractional distribution of each of the analytes in the various lipoprotein classes. The LDL and IDL are represented as a single combined fraction (see Materials and Methods for further details). The data represent the mean ± SE of three samples, where each sample is derived from the pooled serum of two mice. Black bars represent C57BL/6J control mice and the white bars the apoE$^{-/-}$ mice.

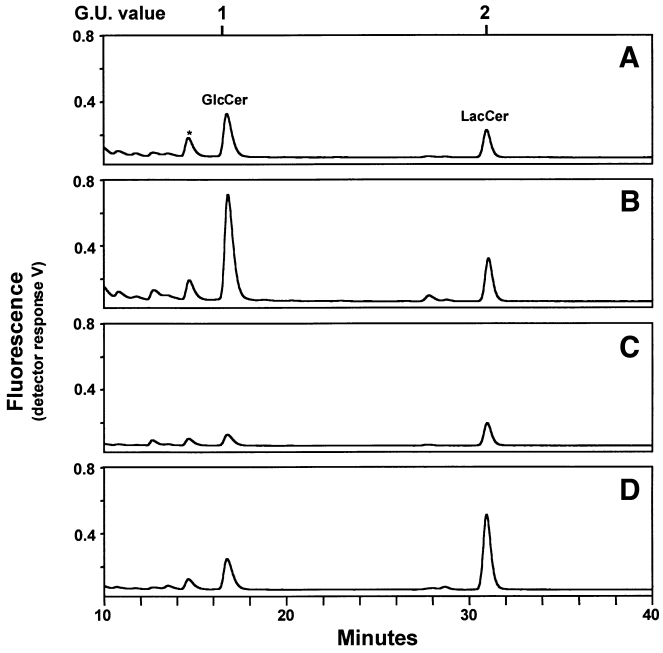

Fig. 8. HPLC analysis of neutral GSLs isolated from mouse aortae. GSLs were isolated by solvent extraction, and the glycan portion was released by ceramide glycanase treatment. The released glycan pool was then 2-AB labeled and analyzed by NP-HPLC. The major GSLs present were identified as GlcCer and LacCer. Neutral GSL profiles of the aortic sinus (A and B) and arch (C and D) of representative C57BL/6J wild-type control (A and C) and apoE$^{-/-}$ (B and D) mice are shown. The asterisk indicates an unidentified compound.

supporting the idea that local synthesis contributes to the GSL levels found in human atherosclerotic plaque. Oxidized LDL has been shown to stimulate GalT-2 transferase activity and LacCer synthesis (56). It is possible that a proportion of the newly synthesized LacCer in the vessel wall might also serve as a precursor for the formation of gangliosides in this tissue. Regardless of the origins of the accumulated GSLs in the vessel wall, in vitro studies imply that the overall biological effect would be to promote atherosclerosis, for example, by stimulating smooth muscle cell proliferation in the case of LacCer and by stimulating foam cell formation in the case of GM3 (30, 31).

The profile of artery wall gangliosides determined in our studies indicates that, in the non-diseased vessels (both the sinus and arch), GM3, GM2, and GM1 are the most abundant gangliosides. Interestingly, in the atherosclerotic tissue, glycolyl GM2 also makes a significant contribution (Fig. 9). Because there is little evidence that vessel wall cells constitutively synthesize glycolyl neuraminic acid, and because this ganglioside is only present in trace amounts in healthy aortae, one interpretation is that the presence of glycolyl GM2 in the diseased tissue may reflect the GSL composition of macrophage foam cells. Analogous observations have been made where tumor-infiltrating macrophages were found to alter dramatically the ganglioside composition of murine brain (57). Of possible significance, murine macrophages have the capacity to produce a spectrum of gangliosides, including glycolyl GM2, GM1b, and GD1a (57, 58). It is also likely that lipoprotein-derived glycolyl GM2 contributes to the increased ganglioside levels observed in the atherosclerotic lesion (20). Infiltrating monocytes that have differentiated to macrophages could utilize both lipoprotein-derived and locally synthesized GSLs to form new gangliosides. An example of the latter could be the formation of GD1a from GM3 via the following pathway: GM3→GM2→GM1a→GD1a (57, 58).

The finding that GD3, but not LacCer, appears to accumulate in the aortic sinus of the apoE$^{-/-}$ mice is consis-

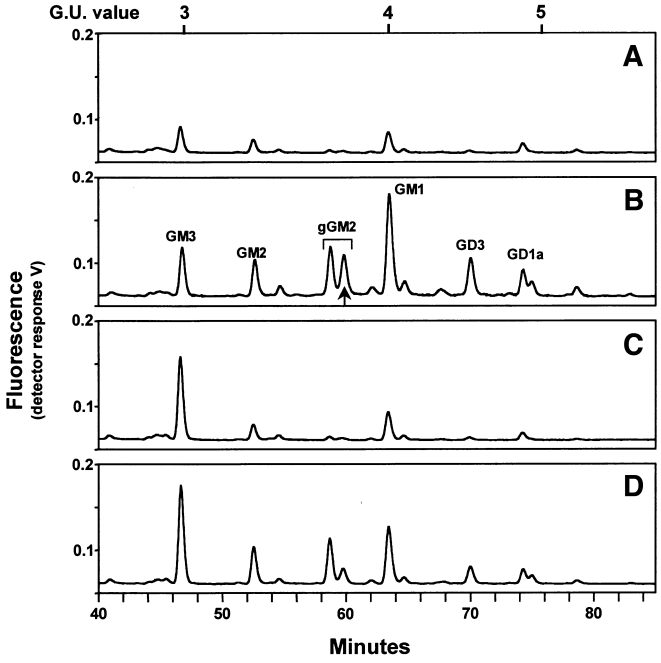

Fig. 9. HPLC analysis of gangliosides isolated from mouse aortae. Gangliosides were isolated by solvent extraction, and the glycan portion was released by ceramide glycanase treatment. The released glycan pool was then 2-AB labeled and analyzed by NP-HPLC. The major gangliosides present were identified as GM3, GM2, glycolyl GM2, GM1, GD3, and GD1a. Ganglioside profiles of the aortic sinus (A and B) and arch (C and D) of representative C57BL/6J wild-type control (A and C) and apoE$^{-/-}$ (B and D) mice are shown. The arrow indicates a compound that was tentatively assigned as glycolyl GM2 lactone.

tent with the idea that there could be regional differences in the mechanisms of atherosclerosis development. It is possible that Gal T-2 transferase activity (which catalyzes the formation of LacCer from GlcCer) is specifically upregulated in the smooth muscle cells of the aortic arch, but not in the aortic sinus. Differences in the cellular composition of the vessel wall at different stages of atherosclerosis may also underlie the altered GSL profiles observed as the severity of disease increases (25).

Site-specific differences in lesion development in the apoE$^{-/-}$ mouse have been observed (43). Unexpectedly, the lipid-lowering drug probucol was found to increase lesion size in the aortic root, but to inhibit lesion size in the aortic arch (43). Hypothetical explanations for site-specific differences in the effects of probucol on lesion development could also be considered relevant in terms of site-specific mechanisms of atherogenesis per se (e.g., hemodynamic factors) and have been discussed previously (43).

Studies of human atherosclerotic tissue indicate that the accumulation of GSL in the artery wall is selective and site specific (25). For example, compared with control tissue, GD3 levels are dramatically decreased in the intima and increased in the media of lesions (25). Our studies represent an overall picture of GSL accumulation. "Normal" regions of the aortic arch, as dissected in our work,

TABLE 2. Cholesterol and glycolipid levels in C57BL/6J and apoE$^{-/-}$ mouse aortic tissue

	Arch		Sinus	
	C57BL/6J	ApoE$^{-/-}$	C57BL/6J	ApoE$^{-/-}$
Tissue mass[a]	2.12 ± 0.16	2.03 ± 0.24	0.54 ± 0.16	1.33 ± 0.18[c]
Cholesterol[b]	5.5 ± 0.4	10.6 ± 0.3[e]	4.3 ± 0.4	15.0 ± 2.2[d]
Gangliosides[b]	0.67 ± 0.08	1.00 ± 0.05[c]	0.38 ± 0.09	1.37 ± 0.13[e]
GlcCer[b]	0.32 ± 0.05	1.14 ± 0.29[c]	0.43 ± 0.06	0.66 ± 0.13
LacCer[b]	0.35 ± 0.07	2.20 ± 0.92	0.35 ± 0.08	0.38 ± 0.03

Data are means ± SE, n = three mice analysed for all compounds. Statistical significance was determined using the Student's *t*-test.

[a] Values are mg wet weight.

[b] Values are nmol.

[c] $P < 0.05$.

[d] $P < 0.001$.

[e] $P < 0.01$,

would make a significant contribution to the diseased tissue GSLs analyzed, because lesions were not as severe as can be induced by feeding a high fat diet. It is also interesting to note that whereas total ganglioside levels were increased more in the aortic sinus than arch (360% vs. 49% increase, respectively), the concentration of LacCer was not significantly increased in the aortic sinus. This could indicate that in the sinus, LacCer is used as a substrate for

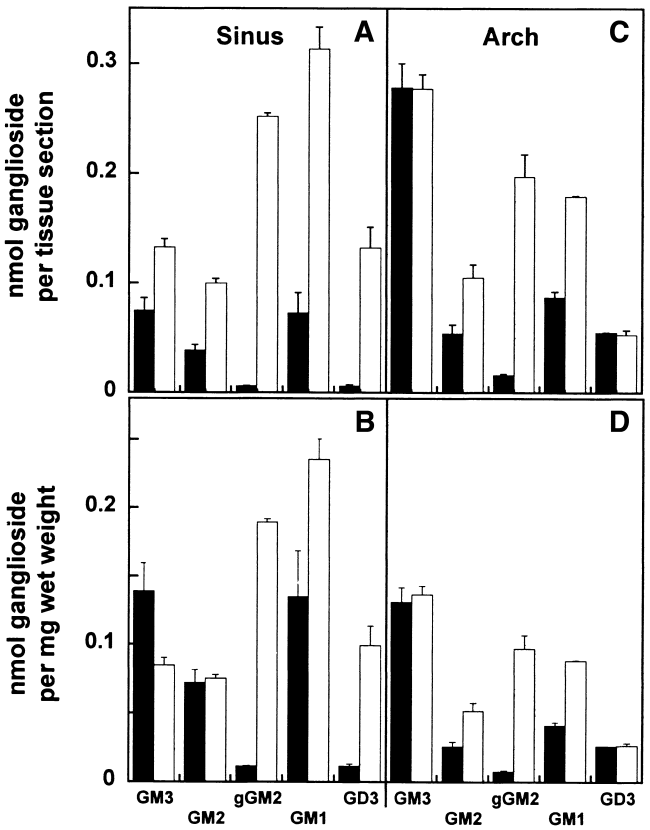

Fig. 10. Aortic ganglioside composition. The relative concentrations of individual gangliosides, identified as illustrated in Fig. 9, are represented by each of the bars in the histograms. The ganglioside composition of the aortic sinus (A and B) and arch (C and D) are shown for both the C57BL/6J control (black bars) and apoE$^{-/-}$ (white bars) mice. Data are means ± SE, n = 3.

ganglioside synthesis or that in the arch, gangliosides are degraded. Studies of glycosyl transferase activity in the various tissues would be required to investigate this proposal.

In vitro studies indicate that GSLs can play an important role in cell biology, for example, in the modulation of transmembrane signaling (35, 59). Although in vitro studies also point toward a proatherogenic role for GSLs (56, 60), it should be emphasized that there is no evidence that, in an animal model, disease progression can be modulated via selective manipulation of GSL metabolism by pharmacological interventions or genetic manipulations. The use of the apoE$^{-/-}$ mouse may help to bridge this gap in understanding the potential role of GSLs in atherogenesis.

In conclusion, the present study shows that, in the apoE$^{-/-}$ mouse, there is an increase in the serum concentrations of both neutral and charged GSLs, a redistribution of these GSLs from HDL to VLDL particles, and an accumulation of specific GSLs in atherosclerosis-prone regions of the aorta. These observations are in concordance with the observations that plasma and artery wall GSL concentrations are increased in humans who are at increased risk for the development of atherosclerosis or who have clinically established atherosclerosis (20–29). The apoE$^{-/-}$ mouse, therefore, provides a convenient animal model to study the potential role of GSLs in atherogenesis.

Mr. David Smith is thanked for his expert assistance in the animal procedures. Prof. Raymond Dwek is thanked for his support. This work was supported by a Wellcome Trust fellowship and grant (058833) awarded to B.G. and by the National Health and Medical Research Council of Australia (R.S.). F.M.P. is a Lister Institute Research Fellow. We thank Dr. Robert Bateman and Dr. Richard Tyldesley of Micromass Ltd. for access to the MALDI-Q-Tof mass spectrometer.

Manuscript received 9 August 2001 and in revised form 31 October 2001.

REFERENCES

1. Breslow, J. L. 1996. Mouse models of atherosclerosis. *Science.* **272:** 685–688.
2. Plump, A. S., J. D. Smith, T. Hayek, K. Aalto-Setala, A. Walsh, J. G. Verstuyft, E. M. Rubin, and J. L. Breslow. 1992. Severe hypercholesterolemia and atherosclerosis in apolipoprotein E-deficient mice created by homologous recombination in ES cells. *Cell.* **71:** 343–353.
3. Zhang, S. H., R. L. Reddick, J. A. Piedrahita, and N. Maeda. 1992. Spontaneous hypercholesterolemia and arterial lesions in mice lacking apolipoprotein E. *Science.* **258:** 468–471.
4. Reddick, R. L., S. H. Zhang, and N. Maeda. 1994. Atherosclerosis in mice lacking apo E. Evaluation of lesional development and progression. *Arterioscler. Thromb.* **14:** 141–147.
5. Nakashima, Y., A. S. Plump, E. W. Raines, J. L. Breslow, and R. Ross. 1994. ApoE-deficient mice develop lesions of all phases of atherosclerosis throughout the arterial tree. *Arterioscler. Thromb.* **14:** 133–140.
6. Tamminen, M., G. Mottino, J. H. Qiao, J. L. Breslow, and J. S. Frank. 1999. Ultrastructure of early lipid accumulation in ApoE-deficient mice. *Arterioscler. Thromb. Vasc. Biol.* **19:** 847–853.
7. Zhou, X., S. Stemme, and G. K. Hansson. 1996. Evidence for a local immune response in atherosclerosis. CD4+ T cells infiltrate lesions of apolipoprotein-E-deficient mice. *Am. J. Pathol.* **149:** 359–366.
8. Palinski, W., V. A. Ord, A. S. Plump, J. L. Breslow, D. Steinberg, and J. L. Witztum. 1994. ApoE-deficient mice are a model of lipoprotein oxidation in atherogenesis: demonstration of oxidation-specific epitopes in lesions and high titers of autoantibodies to malondialdehyde-lysine in serum. *Arterioscler. Thromb.* **14:** 605–616.
9. Hayek, T., J. Oiknine, J. G. Brook, and M. Aviram. 1994. Increased plasma and lipoprotein lipid peroxidation in apo E-deficient mice. *Biochem. Biophys. Res. Commun.* **201:** 1567–1574.
10. Letters, J. M., P. K. Witting, J. K. Christison, A. W. Eriksson, K. Pettersson, and R. Stocker. 1999. Time-dependent changes to lipids and antioxidants in plasma and aortas of apolipoprotein E knockout mice. *J. Lipid Res.* **40:** 1104–1112.
11. Smith, J. D., E. Trogan, M. Ginsberg, C. Grigaux, J. Tian, and M. Miyata. 1995. Decreased atherosclerosis in mice deficient in both macrophage colony-stimulating factor (op) and apolipoprotein E. *Proc. Natl. Acad. Sci. USA.* **92:** 8264–8268.
12. Zhou, X., A. Nicoletti, R. Elhage, and G. K. Hansson. 2000. Transfer of CD4(+) T cells aggravates atherosclerosis in immunodeficient apolipoprotein E knockout mice. *Circulation.* **102:** 2919–2922.
13. Dong, Z. M., A. A. Brown, and D. D. Wagner. 2000. Prominent role of P-selectin in the development of advanced atherosclerosis in ApoE-deficient mice. *Circulation.* **101:** 2290–2295.
14. Osada, J., J. Joven, and N. Maeda. 2000. The value of apolipoprotein E knockout mice for studying the effects of dietary fat and cholesterol on atherogenesis. *Curr. Opin. Lipidol.* **11:** 25–29.
15. Thomas, S. R., S. B. Leichtweis, K. Pettersson, K. D. Croft, T. A. Mori, A. J. Brown, and R. Stocker. 2001. Dietary cosupplementation with vitamin E and coenzyme Q(10) inhibits atherosclerosis in apolipoprotein E gene knockout mice. *Arterioscler. Thromb. Vasc. Biol.* **21:** 585–593.
16. Kundu, S. K., I. Diego, S. Osovitz, and D. M. Marcus. 1985. Glycosphingolipids of human plasma. *Arch. Biochem. Biophys.* **238:** 388–400.
17. Senn, H. J., S. Sellin, E. Fitzke, T. Stehle, D. Haussinger, H. Wieland, and W. Gerok. 1992. Biosynthesis and excretion of gangliosides by the isolated perfused rat liver. *Eur. J. Biochem.* **205:** 809–814.
18. Senn, H. J., M. Orth, E. Fitzke, H. Wieland, and W. Gerok. 1989. Gangliosides in normal human serum: concentration, pattern and transport by lipoproteins. *Eur. J. Biochem.* **181:** 657–662.
19. Loeb, J. A., and G. Dawson. 1982. Reversible exchange of glycosphingolipids between human high and low density lipoproteins. *J. Biol. Chem.* **257:** 11982–11987.
20. Bobryshev, Y. V., R. S. Lord, N. K. Golovanova, E. V. Gracheva, N. D. Zvezdina, V. L. Sadovskaya, and N. V. Prokazova. 1997. Incorporation and localisation of ganglioside GM3 in human intimal atherosclerotic lesions. *Biochim. Biophys. Acta.* **1361:** 287–294.
21. Bobryshev, Y. V., R. S. Lord, N. K. Golovanova, E. V. Gracheva, N. D. Zvezdina, and N. V. Prokazova. 2001. Phenotype determination of anti-GM3 positive cells in atherosclerotic lesions of the human aorta: hypothetical role of ganglioside GM3 in foam cell formation. *Biochim. Biophys. Acta.* **1535:** 87–99.
22. Senn, H. J., M. Orth, E. Fitzke, W. Koster, H. Wieland, and W. Gerok. 1992. Human serum gangliosides in hypercholesterolemia, before and after extracorporeal elimination of LDL. *Atherosclerosis.* **94:** 109–117.
23. Mukhin, D. N., N. V. Prokazova, L. D. Bergelson, and A. N. Orekhov. 1989. Ganglioside content and composition of cells from normal and atherosclerotic human aorta. *Atherosclerosis.* **78:** 39–45.
24. Mukhin, D. N., and N. V. Prokazova. 1992. Neutral glycosphingolipid content and composition of cells from normal and atherosclerotic human aorta. *Atherosclerosis.* **93:** 173–177.
25. Mukhin, D. N., F. F. Chao, and H. S. Kruth. 1995. Glycosphingolipid accumulation in the aortic wall is another feature of human atherosclerosis. *Arterioscler. Thromb. Vasc. Biol.* **15:** 1607–1615.
26. Chatterjee, S. B., S. Dey, W. Y. Shi, K. Thomas, and G. M. Hutchins. 1997. Accumulation of glycosphingolipids in human atherosclerotic plaque and unaffected aorta tissues. *Glycobiology.* **7:** 57–65.
27. Breckenridge, W. C. 1977. Structural characterization of gangliosides from normal and atherosclerotic human thoracic aortas. *Adv. Exp. Med. Biol.* **82:** 164–166.
28. Breckenridge, W. C., J. L. Halloran, K. Kovacs, and M. D. Silver. 1975. Increase of gangliosides in atherosclerotic human aortas. *Lipids.* **10:** 256–259.
29. Garner, B., D. J. Harvey, L. Royle, M. Frischmann, F. Nigon, M. J. Chapman, and P. M. Rudd. 2001. Characterisation of human apolipoprotein B100 oligosaccharides in low density lipoprotein (LDL) subfractions derived from normal and hyperlipidemic plasma:

deficiency of α-*N*-acetylneuraminyllactosyl ceramide in light and small dense LDL. *Glycobiology.* **11:** 791–802.
30. Chatterjee, S. 1991. Lactosylceramide stimulates aortic smooth muscle cell proliferation. *Biochem. Biophys. Res. Commun.* **181:** 554–561.
31. Prokazova, N. V., I. A. Mikhailenko, and L. D. Bergelson. 1991. Ganglioside GM3 stimulates the uptake and processing of low density lipoproteins by macrophages. *Biochem. Biophys. Res. Commun.* **177:** 582–587.
32. Wen, F. Q., A. A. Jabbar, D. A. Patel, T. Kazarian, and L. A. Valentino. 1999. Atherosclerotic aortic gangliosides enhance integrin-mediated platelet adhesion to collagen. *Arterioscler. Thromb. Vasc. Biol.* **19:** 519–524.
33. Hakomori, S. 1990. Bifunctional role of glycosphingolipids: modulators for transmembrane signaling and mediators for cellular interactions. *J. Biol. Chem.* **265:** 18713–18716.
34. Yatomi, Y., Y. Igarashi, and S. Hakomori. 1996. Effects of exogenous gangliosides on intracellular Ca2+ mobilization and functional responses in human platelets. *Glycobiology.* **6:** 347–353.
35. Hakomori, S., and Y. Igarashi. 1995. Functional role of glycosphingolipids in cell recognition and signaling. *J. Biochem.* **118:** 1091–1103.
36. Ryan, J. L., L. Gobran, and D. C. Morrison. 1986. Modulation of murine macrophage metabolism by glycolipids: inhibition of LPS-induced metabolism by specific gangliosides. *J. Leukoc. Biol.* **40:** 367–379.
37. Nojiri, H., F. Takaku, Y. Terui, Y. Miura, and M. Saito. 1986. Ganglioside GM3: an acidic membrane component that increases during macrophage-like cell differentiation can induce monocytic differentiation of human myeloid and monocytoid leukemic cell lines HL- 60 and U937. *Proc. Natl. Acad. Sci. USA.* **83:** 782–786.
38. Miles, L. A., C. M. Dahlberg, E. G. Levin, and E. F. Plow. 1989. Gangliosides interact directly with plasminogen and urokinase and may mediate binding of these fibrinolytic components to cells. *Biochemistry.* **28:** 9337–9343.
39. Coleman, D. L., D. C. Morrison, and J. L. Ryan. 1986. Gangliosides block the inhibition of macrophage Fc-dependent phagocytosis by lipopolysaccharide. *Cell. Immunol.* **100:** 288–299.
40. Ding, Y., K. Ma, and Z. C. Tsui. 1998. Induction of nitric oxide production by ganglioside GM3 in murine peritoneal macrophages activated for tumor cytotoxicity. *In Vivo.* **12:** 357–361.
41. Simons, M., T. Friedrichson, J. B. Schulz, M. Pitto, M. Masserini, and T. V. Kurzchalia. 1999. Exogenous administration of gangliosides displaces GPI-anchored proteins from lipid microdomains in living cells. *Mol. Biol. Cell.* **10:** 3187–3196.
42. Li, R., J. Manela, Y. Kong, and S. Ladisch. 2000. Cellular gangliosides promote growth factor-induced proliferation of fibroblasts. *J. Biol. Chem.* **275:** 34213–34223.
43. Witting, P. K., K. Pettersson, J. Letters, and R. Stocker. 2000. Site-specific antiatherogenic effect of probucol in apolipoprotein E-deficient mice. *Arterioscler. Thromb. Vasc. Biol.* **20:** E26–E33.
44. Neuzil, J., J. K. Christison, E. Iheanacho, J. C. Fragonas, V. Zammit, N. H. Hunt, and R. Stocker. 1998. Radical-induced lipoprotein and plasma lipid oxidation in normal and apolipoprotein E gene knockout (apoE−/−) mice: apoE−/− mouse as a model for testing the role of tocopherol-mediated peroxidation in atherogenesis. *J. Lipid Res.* **39:** 354–368.
45. Sattler, W., D. Mohr, and R. Stocker. 1994. Rapid isolation of lipoproteins and assessment of their peroxidation by high-performance liquid chromatography postcolumn chemiluminescence. *Methods Enzymol.* **233:** 469–489.
46. Zhou, B., S. C. Li, R. A. Laine, R. T. Huang, and Y. T. Li. 1989. Isolation and characterization of ceramide glycanase from the leech, *Macrobdella decora*. *J. Biol. Chem.* **264:** 12272–12277.
47. Guile, G. R., P. M. Rudd, D. R. Wing, S. B. Prime, and R. A. Dwek. 1996. A rapid high-resolution high-performance liquid chromatographic method for separating glycan mixtures and analyzing oligosaccharide profiles. *Anal. Biochem.* **240:** 210–226.
48. Wing, D. R., B. Garner, V. Hunnam, G. Reinkensmeier, U. Andersson, D. J. Harvey, R. A. Dwek, F. M. Platt, and T. D. Butters. 2001. HPLC analysis of ganglioside carbohydrates at the pmol level after ceramide glycanse digestion and fluorerscent labelling with 2-aminobenzamide. *Anal. Biochem.* **298:** 207–217.
49. Yu, R. K., T. A. Koerner, S. Ando, H. C. Yohe, and J. H. Prestegard. 1985. High-resolution proton NMR studies of gangliosides. III. Elucidation of the structure of ganglioside GM3 lactone. *J. Biochem.* **98:** 1367–1373.
50. Riboni, L., R. Ghidoni, and G. Tettamanti. 1989. Formation of ganglioside GD1b-lactone in rat brain from intracisternally administered GD1b. *J. Neurochem.* **52:** 1401–1406.
51. Harvey, D. J., R. H. Bateman, R. S. Bordoli, and R. Tyldesley. 2000. Ionisation and fragmentation of complex glycans with a quadrupole time-of-flight mass spectrometer fitted with a matrix-assisted laser desorption/ionisation ion source. *Rapid Commun. Mass Spectrom.* **14:** 2135–2142.
52. Vance, D. E., and C. C. Sweeley. 1967. Quantitative determination of the neutral glycosyl ceramides in human blood. *J. Lipid Res.* **8:** 621–630.
53. Strasberg, P. M., I. Warren, M. A. Skomorowski, and J. A. Lowden. 1983. HPLC analysis of neutral glycolipids: an aid in the diagnosis of lysosomal storage disease. *Clin. Chim. Acta.* **132:** 29–41.
54. Cotterchio, M., and T. N. Seyfried. 1994. Serum gangliosides in mice with metastatic and non-metastatic brain tumors. *J. Lipid Res.* **35:** 10–14.
55. Kloppel, T. M., T. W. Keenan, M. J. Freeman, and D. J. Morre. 1977. Glycolipid-bound sialic acid in serum: increased levels in mice and humans bearing mammary carcinomas. *Proc. Natl. Acad. Sci. USA.* **74:** 3011–3013.
56. Chatterjee, S. 1998. Sphingolipids in atherosclerosis and vascular biology. *Arterioscler. Thromb. Vasc. Biol.* **18:** 1523–1533.
57. Ecsedy, J. A., H. C. Yohe, A. J. Bergeron, and T. N. Seyfried. 1998. Tumor-infiltrating macrophages influence the glycosphingolipid composition of murine brain tumors. *J. Lipid Res.* **39:** 2218–2227.
58. Yohe, H. C., S. Ye, B. B. Reinhold, and V. N. Reinhold. 1997. Structural characterization of the disialogangliosides of murine peritoneal macrophages. *Glycobiology.* **7:** 1215–1227.
59. Bhunia, A. K., H. Han, A. Snowden, and S. Chatterjee. 1997. Redox-regulated signaling by lactosylceramide in the proliferation of human aortic smooth muscle cells. *J. Biol. Chem.* **272:** 15642–15649.
60. Prokazova, N. V., and L. D. Bergelson. 1994. Gangliosides and atherosclerosis. *Lipids.* **29:** 1–5.